Published in final edited form as:
Brain Res. 2013 June 26; 1518: 91–103. doi:10.1016/j.brainres.2013.04.030.

Striatal oligodendrogliogenesis and neuroblast recruitment are increased in the R6/2 mouse model of Huntington's disease

Mark H. McCollum, **Rebecca T. Leon**, **Daniel B. Rush**, **Kathleen M. Guthrie**, and **Jianning Wei***
Department of Biomedical Science, Charles E. Schmidt College of Medicine, Florida Atlantic University, 777 Glades Road, Boca Raton, FL 33431, USA

Abstract

The subventricular zone (SVZ) is one of the two major neurogenic regions in the adult mammalian brain. Its close proximity to the striatum suggests that a cell-based therapeutic strategy for the treatment of Huntington's disease (HD) is possible. To achieve this, it is important to understand how adult cell production, migration and differentiation may be altered in the HD brain. In this study, we quantified the number of adult-born striatal cells and characterized their fate in the R6/2 transgenic mouse model of HD. We found that the number of new striatal cells was approximately two-fold greater in R6/2 versus wild type mice, while SVZ cell proliferation was not affected. Using cell-type specific markers, we demonstrated that the majority of new striatal cells were mature oligodendrocytes or oligodendroglial precursors that were intrinsic to the striatum. We also detected a significant increase in the number of migrating neuroblasts that appeared to be recruited from the SVZ to the striatum. However, these neuroblasts did not mature into neurons and most were lost between 1 and 2 weeks of cell age. Crossing the R6/2 mice with mice over-expressing brain-derived neurotrophic factor in the striatum increased the numbers of neuroblasts that survived to 2 weeks, but did not promote their differentiation. Together, our data indicate that the potential treatment of HD based on manipulating endogenous progenitor cells should take into consideration the apparent enhancement in striatal oligodendrogliogenesis and the limited ability of recruited SVZ neuroblasts to survive long-term and differentiate in the diseased striatum.

Keywords

Huntington's disease; adult neurogenesis; oligodendroglia; neuroblast; brain derived neurotrophic factor

1. Introduction

Huntington's Disease (HD) is a fatal inherited neurodegenerative disease caused by a mutation in the huntingtin gene and characterized by the progressive loss of striatal GABAergic medium spiny neurons (MSNs), which constitute 95% of striatal neurons (Reiner et al., 1988). Therapeutic replacement of MSNs thus represents a potential strategy for treating HD (Benraiss and Goldman, 2011). Persistent neurogenesis occurs in the adult

*Corresponding author at: Tel: (01) 561-297-0002, Fax: (01) 561-297-2221, jwei@fau.edu.

mammalian (including human) brain within the subventricular zone (SVZ) lining the lateral ventricles and in the subgranular zone of the hippocampus (Eriksson et al., 1998; Zhao et al., 2008). In these neurogenic regions, resident stem cells give rise to new neurons throughout life. In addition to playing a critical role in neuronal plasticity in the normal brain, there is increasing evidence that adult neurogenesis is modulated by and responsive to brain injuries and diseases (Arvidsson et al., 2002; Curtis et al., 2007; Kernie and Parent, 2010; Ohira, 2011; Winner et al., 2011). Brain insult can stimulate the proliferation of SVZ neural progenitors and adult born neuroblasts can then migrate to damaged sites, where some reportedly differentiate into functional neurons within adult brain circuits (Chmielnicki et al., 2004; Tattersfield et al., 2004). This raises the intriguing possibility that neurogenic regions may be manipulated to generate replacement neurons in damaged areas of the adult brain (Lie et al., 2004; Gil-Mohapel et al., 2011; Saha et al., 2012).

The progressive nature of the classical neurodegenerative diseases, including HD, makes these pathologies ideal candidates for targeted enhancement of endogenous neurogenesis. Unlike traumatic brain injury or stroke, where massive losses of neurons occur rapidly, neurodegenerative diseases are characterized by the gradual losses of neurons over the course of years or decades. Therefore, it is possible that the slow rate of neuronal loss may be abated by neuronal replacement overtime, even if this is limited. The close proximity of the degenerating striatum to the neurogenic SVZ suggests a therapeutic strategy for HD based on exploiting this nearby neural stem cells. Under normal physiological conditions, the vast majority of neuroblasts generated in the SVZ migrate to the olfactory bulb in the rostral migratory stream (Ming and Song, 2005). However, it has been shown that intraventricular administration of growth factors, or manipulations that increase growth factor availability in striatum, can stimulate SVZ-derived neuroblasts to migrate instead into the adjacent striatum and mature into neurons in HD mouse models, with beneficial effects that manifest as a slowing of disease progression (Pencea et al., 2001; Chmielnicki et al., 2004; Cho et al., 2007; Gharami et al., 2008). Furthermore, the heritable basis of HD lends itself to early intervention before the onset of debilitating symptoms. The quality of life for HD patients may be substantially improved by even a modest abatement of neuronal loss through the regenerative potential of endogenous neural progenitors. In addition to its clinical potential, adult neurogenesis has also been implicated in the pathogenesis of HD and other neurodegenerative diseases (Phillips et al., 2005; Winner et al., 2011). Therefore, the study of adult neurogenesis is important for understanding the pathophysiology of these diseases in addition to therapeutic implications.

SVZ and hippocampal neurogenesis in HD animal models have been extensively studied. Using the 5-bromo-2-deoxyuridine (BrdU) labeling approach, it has been showing by most studies that hippocampal neurogenesis is reduced in commonly used transgenic HD mouse models, including R6/2 (Phillips et al., 2005), R6/1 (Lazic et al., 2004; 2006) and YAC128 mice (Simpson et al., 2011). However, no significant changes in SVZ neurogenesis have been found in these mouse models (Lazic et al., 2004; Phillips et al., 2005; Gil-Mohapel et al., 2011; Simpson et al., 2011). On the other hand, increased cell proliferation and neurogenesis was found in the subependymal layer of adult human HD brain using endogenous mitotic marker proliferating cell nuclear antigen (PCNA) (Curtis et al., 2003). Despite of these important findings, cell proliferation within HD-affected striatum has received less attention and has not been systemically analyzed. In the present study, we investigated striatal cell proliferation and survival in the R6/2 transgenic mouse model of HD. This strain expresses exon 1 of the human huntingtin gene, containing ~160 CAG repeats (Mangiarini et al., 1996). We utilized the mitotic cell marker 5-bromo-2-deoxyuridine (BrdU) to label and quantify adult-born cells in both the SVZ and striatum of R6/2 and WT mice. The phenotypic fate of new striatal cells was characterized using cell-type specific markers. Our data demonstrate that the numbers of BrdU-positive ($BrdU^+$)

cells are significantly increased in the striatum of R6/2 mice, and that the majority of these cells are oligodendrocytes and oligodendroglial progenitor cells (OPCs) arising within the striatum. A small number of $BrdU^+$ cells in the R6/2 striatum are migrating neuroblasts derived from the SVZ. We also tested the effect of supplying brain derived neurotrophic factor (BDNF) on striatal neurogenesis in R6/2 mice by crossing the R6/2 mice with a transgenic strain overexpressing BDNF.

2. Results

2.1 Adult R6/2 mice exhibit increased numbers of $BrdU^+$ cells in striatum but no change in SVZ cell proliferation

We first sought to investigate whether striatal neurogenesis is altered in R6/2 mice compared to WT littermates. To ensure that infrequently dividing precursor cells would be labeled, animals at 5 weeks old received daily injections of BrdU (50 mg/kg, i.p.) for 4 weeks. Two weeks after the last injection, brains from mice at 11 weeks of age were collected for immunofluorescence analysis (Fig. 1A). By this time, R6/2 mice showed distinct motor symptoms and weight loss. Immunostaining revealed a significant increase in the number of $BrdU^+$ cells in the striatum of R6/2 mice compared to WT animals (Fig. 2A). The mean density of BrdU-labeled nuclei in the striatum of R6/2 mice (4540 ± 289 cells/mm^3 , n=5) at this time was approximately twice that of new striatal cells in WT controls (2488 ± 437 cells/mm^3, n=4, p=0.0048) (Fig. 2B). Notably, these $BrdU^+$ cells were evenly distributed throughout the striatum in both genotypes.

To determine if the increase in $BrdU^+$ cells in the striatum resulted from enhanced SVZ cell proliferation and later migration to striatum, we quantified numbers of BrdU-labeled nuclei in the SVZ at 1 hour after BrdU administration in 9-week-old mice (Fig. 1B). Although we detected a few $BrdU^+$ cells in the striatum at this time point, the vast majority of $BrdU^+$ cells were restricted to the SVZ (Fig. 2C), suggesting that proliferative cells in the striatum are more quiescent than progenitors in the SVZ. Quantitative analysis indicated no significant difference in SVZ cell proliferation between 9-week-old WT and R6/2 mice (Fig. 2D, WT: 1008.3 ± 110.2 cells/mm^2 , R6/2: 1153.2 ± 94.6 cells/mm^2 , n=3 for each group, p=0.37). In addition, we also examined the SVZ at 4 days post-BrdU treatment (Fig. 1B). The number of $BrdU^+$ cells in the SVZ of R6/2 mice (551.8 ± 37.1 cells/mm^2, n=3) was similar to that of WT mice at 4 days post-BrdU treatment (511.2 ± 45.2 cells/mm^2 , n=3) (Fig. 2D). As expected, the density of labeled SVZ cells in both genotypes had decreased, while numbers in the RMS were obviously increased, indicating that most newborn cells rapidly migrated out of the SVZ. The density of $BrdU^+$ cells in the SVZ of WT mice at 4 days was approximately 50% of the density at 1-hour post-BrdU treatment (Fig. 2D).

2.2 Most newborn cells in the striatum of R6/2 and WT mice are $Olig2^+$ cells

We next used cell-type specific markers to identify the phenotypes of new cells in the striatum of 11 week-old R6/2 and WT mice after long-term BrdU treatment. We did not detect any $BrdU^+$ cells that co-expressed the neuronal marker, NeuN, in either genotype, indicating that the increase in BrdU-labeled cells did not represent net neurogenesis in terms of $NeuN^+$ cells. Orthogonal views of stained cells demonstrated that occasional nuclei that appeared “co-labeled” by BrdU and NeuN antibodies were actually closely adjacent cells (Fig. 3A–B for R6/2 mice, images of WT not shown). The majority of $BrdU^+$ cells in the striatum of R6/2 and WT mice were in fact immunoreactive for oligodendrocyte lineage transcription factor 2 (Olig2), a marker for mature oligodendrocytes and proliferating OPCs (Clarke et al., 2012) (Fig. 3C–D for R6/2 mice, images of WT mice not shown). $BrdU^+$ neuroblasts were also identified in the striatum of both genotypes at this time, as defined by cytoplasmic expression of DCX in the cell soma and at least one well-defined process as

illustrated in Fig. 3E–F in R6/2 mice. Striatal neuroblasts were often proximal to the SVZ and appeared in small clusters. Much less frequently, $BrdU^+$ cells were also positive for the astrocytic marker glial fibrillary acidic protein (GFAP), the microglial marker Iba1 or the mature astrocyte marker S100β in both R6/2 and WT mice (images not shown).

We estimated the percentage of each BrdU-labeled cell type in the striatum, and determined that approximately 80% of $BrdU^+$ cells derived from the oligodendrocyte lineage and were $Olig2^+$ in both genotypes, although the overall number of $BrdU^+/Olig2^+$ cells in R6/2 mice is greater than that of WT mice. DCX^+ cells constitute 2.4% and 3.7% of $BrdU^+$ cells in WT and R6/2 mice, respectively. Microglia and astrocytes are too rare to quantify. We estimated that other cell phenotypes, including microglia, astrocytes and unknown cell types, accounted for ~15% of all $BrdU^+$ cells (Fig. 3G), with no significant difference between WT and R6/2 mice, suggesting that the fate determination within these glial populations are not altered in R6/2 mice.

2.3 $Olig2^+$ cells are either mature or immature oligodendrocytes and arise within the striatum

We next determined whether striatal $BrdU^+/Olig2^+$ cells were mature or immature oligodendrocytes in 11-week-old R6/2 and WT mice. Newly formed myelinating, mature oligodendrocytes were stained with 2,3-cyclic nucleotide 3-phosphodiesterase (CNPase), a marker for myelin (Fig. 4A). The other $BrdU^+$ cells co-expressed NG2 chondroitin sulfate proteoglycan, a marker closely associated with OPCs (Richardson et al., 2011) and for proliferating cell nuclear antigen (PCNA), a marker of actively dividing cells (Fig. 4B). We further analyzed the percentage of $NG2^+$ and $CNPase^+$ cells in $BrdU^+$ cells (Fig. 4C). It is apparent that $NG2^+$ cells represent a larger portion of $BrdU^+$ cells in both WT and R6/2 mice (Fig. 4C). Moreover, R6/2 mice appear to have more mature striatal oligodendrocytes; however, this did not reach to statistical significance (p=0.15, n=3 for WT and n=4 for R6/2).

To further track the development of these $Olig2^+$ cells, we examined co-localization of BrdU and Olig2 at different time points after BrdU pulse labeling. We detected $BrdU^+/(Olig2^+$ cells as early as 1 hour after pulse labeling in both WT and R6/2 mice (219.7 ± 35.1 cells/striatum for WT mice *vs.* 296.5 ± 47.1 cells/ striatum for R6/2 mice, n=3). Notably, there was significant increase in numbers of new oligodendroglial cells in R6/2 versus WT mice at 7 days after BrdU administration (213.3 ± 14.9 cells/striatum for WT mice *vs.* 345.6 ± 19.6 cells/ striatum for R6/2 mice *p<0.01, n=3, Fig. 5A). However, by 14 days after BrdU administration, the number of co-labeled cells in R6/2 mice was reduced by more than half (#p<0.01, Fig. 5A) and had declined to a smaller extent in WT mice as well. This could indicate an up-regulation of oligodendrogliogenesis in the striatum of R6/2 mice in a microenvironment that does not sustain their prolonged survival. To evaluate the distribution of $BrdU^+/ Olig2^+$ cells in the striatum, we measured the distances of labeled cells from the lateral ventricle (LV) and from the corpus callosum (CC). Double-labeled cells were widely distributed in the striatum even at 1-hour post-BrdU labeling (Fig. 5B), making it unlikely these cells migrated into the striatum from the SVZ. Thus, the increase in oligodendroglial cells in R6/2 mice is likely the result of stimulated proliferation of OPCs native to the striatum.

2.4 Striatal neuroblasts are increased in R6/2 mice and originate from the SVZ

We estimated the number of striatal DCX^+ cells in R6/2 and WT mice at 9 weeks of age and found that striatal neuroblasts were approximately two-fold more numerous in R6/2 mice (156.3 ± 10.2 cells/striatum, n=12) compared to WT mice (67.2 ± 6.8 cells/striatum, n=12) (Fig. 6A). To monitor the survival and development of DCX^+ cells in the striatum, we

estimated the percentage of $BrdU^+$ cells that co-express DCX at multiple time points after BrdU pulse labeling. As expected, $BrdU^+/DCX^+$ cells in the striatum were very rare at 1 hour after BrdU treatment in mice of both genotypes (<3% of $BrdU^+$ cells, Fig. 6B). By 4 days, the percentage of striatal neuroblasts that were co-labeled with BrdU was highest (~15% in R6/2 mice). It declined between 4 and 7 days (~12% in R6/2 mice at 7 days), but was greatly reduced by 14 days (~4% of all $BrdU^+$ cells in R6/2 mice) (Fig. 6B). We did not detect any cells that co-expressed BrdU and NeuN at 14 days, making it unlikely that these DCX^+ cells differentiated into mature neurons. Additionally, although a few neuroblasts were observed deep in the striatal parenchyma, we found that most DCX^+ cells in R6/2 and WT mice were either clustered near the SVZ or along the RMS/CC (within 500 μm of one of these structures) (Fig. 6C–D). This distribution suggests that the majority of $BrdU^+$ neuroblasts migrated to the striatum from these neurogenic regions. This is also consistent with our observation that $DCX^+/BrdU^+$ cells were rarely detected after 1-hour post-BrdU labeling due to insufficient time for cells to migrate from SVZ or RMS.

Although these DCX+ cells did not develop into mature NeuN+ neurons, it is possible that they can mature into early post-mitotic neurons. To test this possibility, we included a cell-specific marker for early post-mitotic neurons, calretinin (CR), in our studies (Brandt et al., 2003). We could detect CR^+ striatal cells in WT and R6/2 mice 14 days post BrdU treatment and most of these CR^+ cells localized along the RMS/CC. However, we could not detect any CR^+ cells that co-localized with BrdU in the striatum (Supplementary Fig. S1A). To exclude the possibility that the amount of BrdU delivered in the pulse-labeling experiment is not sufficient to label CR^+ cells, we also performed CR/BrdU co-labeling in brain samples after long-term BrdU treatment. Similarly, we could not detect any CR^+/BrdU cells (Supplementary Fig. S1B). As a comparison, we can easily detect $CR^+/BrdU^+$ cells in the SGZ region in R6/2 mice 14 days post BrdU injection (Supplementary Fig. S1C). Therefore, it is not clear about the identity of these CR^+ cells in the striatum. As expected, we could not detect any newly formed $calbindin^+$ cells, which is a marker for mature neurons (data not shown).

It is therefore very likely that most new neuroblasts we observed in the striatum were 4–7 days old and that many failed survive or develop thereafter, although we can not rule out the possibility that they migrated out of the striatum during this time. Notably, there was no significant difference in the percentage of $BrdU^+/DCX^+$ cells at all time points we examined between WT and R6/2 mice (Fig. 6B), indicating that mutant huntingtin has little effect on fate determination of DCX^+ cells. This apparent short lifespan for adult-born neuroblasts on the diseased striatum is consistent with the limited survival of SVZ-derived neuroblasts reported for another mouse model of progressive striatal degeneration (Luzzati et al., 2011).

2.5 BDNF over-expression increases the number of neuroblasts in the striatum of R6/2 mice

It appears that although there are more DCX^+ cells in the striatum of R6/2 mice, they can only survive for a short time with a significant loss by 14 days. This prompted us to test whether providing them with additional trophic support could further stimulate the recruitment and/or enhance their survival *in vivo*. BDNF supplied by cortical afferents has been established as an important factor for the maintenance of striatal neurons in adults, and reduced levels of striatal BDNF have been demonstrated in both HD patients and animal models (Zuccato et al., 2010). It is thus possible that striatal neuroblasts are not sustained long enough to mature due to the lack of BDNF support in R6/2 striatum. To test if increased endogenous BDNF could promote the recruitment and survival of new neurons in the degenerating striatum, we crossed the R6/2 strain with transgenic mice (BTg) that over-express BDNF throughout forebrain, including the cortex and striatum (Huang et al., 1999). We did notice some behavioral improvements in the crossed mice compared to R6/2 mice

alone, such as a delayed appearance of the hindlimb clasping feature, a well-documented motor dysfunction in R6/2 mice (Mangiarini et al., 1996). The behavioral benefits of elevated BDNF levels in the HD mouse models have been well studied (Canals et al., 2004; Gharami et al., 2008; Xie et al., 2010) and is not the focus of the current study. We then analyzed the number of $BrdU^+$ cells and their co-expression of specific cell markers in WT, R6/2 and BTg:R6/2 mice at 14 days after BrdU pulse labeling at 7 weeks of age.

Our results demonstrate that BTg:R6/2 mice had roughly 2-fold more striatal $BrdU^+$ cells than R6/2 mice (BTg:R6/2: 364.8 ± 166.4 cells, n=4 *vs.* R6/2: 166.4 ± 48.0 cells, n=3, $p<0.01$) (Fig. 7A). Additionally, the number of $BrdU^+$ cells in the SVZ was also significantly enhanced in BTg:R6/2 mice (261.8 ± 6.3 cells/mm^2) compared to R6/2 mice (105.2 ± 8.2 cells/mm^2) (Fig. 7A). There was a trend toward greater numbers of $BrdU^+$/$Olig2^+$ cells in BTg:R6/2 mice (259.2 ± 43.5 cells/striatum) compared to R6/2 mice (130 ± 34.3 cells/striatum), however this difference did not reach statistical significance due to inter-animal variability ($p=0.08$, student's t-test). Moreover, we did not detect an increase in the number of striatal $CNPase^+$/$BrdU^+$ cells in the crossbred animals 14 days post BrdU injection (Supplementary Fig. S2).

Although $Olig^{2+}$ cells still comprised the majority of new cells in the crossed animals as in R6/2 mice, we observed that BDNF over-expression significantly increased the number of striatal DCX^+ neuroblasts (243.2 ± 22.3 cells/striatum, n=4) compared to R6/2 mice (156.3 ± 10.3/striatum, n=12) in the R6/2 model significantly ($p<0.01$, Fig. 7B). More importantly, the percentage of $BrdU^+$ cells that co-expressed DCX was significantly increased in the striatum of BTg:R6/2 mice (12%) compared to R6/2 mice (4%) alone at 14 days post-BrdU administration ($p<0.01$, Fig. 7C), suggesting that BDNF may promote recruitment of DCX^+ cells to striatum and/or survival of adult-born striatal neuroblasts in a normally non-permissive environment. However, we did not detect any $BrdU^+$ cells in striatum that were also immunoreactive for calretinin or NeuN in the crossed mice (data not shown), indicating that increased BDNF did not promote maturation of new striatal neuroblasts during the 14 day survival interval.

3. Discussion

Adult neurogenesis in HD transgenic models has been well studied in both neurogenic regions of the mammalian brain: the dentate gyrus of hippocampus and the SVZ/olfactory bulb system. Reduced hippocampal neurogenesis has been reported in HD animals models and is potentially related to the cognitive abnormalities in HD (Lazic et al., 2004; Gil et al., 2005; Simpson et al., 2011). In contrast, SVZ proliferation has been reported as unchanged in several HD mouse models including R6/2 mice (Lazic et al., 2006; Kohl et al., 2010; Simpson et al., 2011). Consistent with these findings, we did not detect any significant difference in SVZ proliferation between WT and R6/2 mice in the present study.

3.1 Potential role of newborn OPCs and myelinating oligodendrocytes in HD

Neurogenesis in the striatum of HD animal models has not been well examined. A substantial (approximately 10-fold) increase in the number of BrdU cells in the striatum of R6/2 mice at 30 days after $BrdU^+$ administration was reported (Batista et al., 2006). Although a small number of these cells were identified as neuroblasts recruited from the RMS, the phenotypes of the rest of newborn cells were undetermined. In this study, we identified $NG2^+$/$Olig2^+$ OPCs and $CNPase^+$/$Olig2^+$ myelinating oligodendrocytes as the major newborn cell types that are increased in R6/2 mice. To our knowledge, this is the first quantitative analysis of oligodendrogliogenesis in the R6/2 model. Although our quantification is focused on the affected striatum, it is noteworthy to mention that we also noticed an increase of $NG2^+$ cells in other brain areas of R6/2 mice, most prominently in the

corpus collosum and cortex, indicating that the increase of NG2+ cells is not refined to the striatum of R6/2 mice and may have a broader implication._

The functional role of the increased oligodendroglial cells or OPCs in HD is not clear. An intriguing possibility is that oligodendrocytes are recruited to remyelinate degenerating axons in the striatum. It has been reported that the mammalian adult brain responds rapidly to demyelinating insults by regenerating myelinating oligodendrocytes from dividing $NG2^+$ cells (Polito and Reynolds, 2005). Structural magnetic resonance imaging and post-mortem examinations in HD brains suggest that disruptions in white matter integrity resulting myelin breakdown represents an early event in HD pathogenesis (Bartzokis et al., 2007; Rosas et al., 2010; Xiang et al., 2011). Interestingly, an increase in the density of oligodendrocytes in the striatum was demonstrated in presymptomatic HD patient brains years before striatal degeneration (Myers et al., 1991; Gómez-Tortosa et al., 2001). In addition, morphological studies of the corticostriatal circuit in HD patients and animals have supported a “dying back” pattern of degeneration in HD (Han et al., 2010). In this model of neurodegeneration, corticostriatal axons degenerate early in HD and loss of BDNF normally supplied by these axon terminals triggers the subsequent degeneration of MSNs. It is thus possible that oligodendrocyte proliferation may be an important compensatory response to axonal degeneration.

Our data suggest that there are abundant $BrdU^+/NG2^+$ cells in addition to $BrdU^+/CNPase^+$ in the striatum of R6/2 mice. In addition to regenerating oligodendrocytes, there is strong evidence suggesting an important role for NG2-expressing cells in cellular homeostasis, such as responding to neuronally released glutamate (Bergles et al., 2000; Polito and Reynolds, 2005) Importantly, excessive glutamate release has been proposed as an important factor in the striatal cell death observed HD (Paoletti et al., 2008). It is therefore likely that $NG2^+$ cells may respond to excessive glutamate release in HD. It would be interesting to test whether there is any crosstalk between $NG2^+$ cells and mature MSNs in HD and whether it would affect the pathogenesis of HD. Another possible function of $NG2^+$ cells is to provide a favorable substrate to stabilize regenerating axons. In support of this hypothesis, it has been shown that $NG2^+$ cells derived from the adult spinal cord express high levels of laminin and fibronectin and these proteins promote neurite outgrowth on the surface of these cells (Busch et al., 2010).

3.2 Recruitment of neuroblasts to striatum in HD

We found a significant increase in the number of striatal neuroblasts in R6/2 mice, and this is consistent with a recent report in R6/2 mice (Kohl et al., 2010). These neuroblasts are often close to the SVZ or RMS, indicating that they may come from the SVZ neurogenic region. However, we could not detect any of these striatal neuroblasts differentiating into mature neurons. Conversely in the quinolinic acid-based model of HD, it has been reported that migrating neuroblasts enter the affected striatum from the SVZ and some mature into neurons (Tattersfield et al., 2004). This neurogenic effect may result from the dramatic and rapid striatal damage caused by the quinolinic acid toxin. In agreement with this hypothesis, neuroblasts have been shown to migrate into the striatum and differentiate into MSNs 2–4 weeks after transient cerebral artery occlusion (Arvidsson et al., 2002).

Our study on the number of $DCX^+/BrdU^+$ cells at different time intervals after post-BrdU administration suggest that these adult-born striatal neuroblasts may only survive for 4–7 days in both WT and R6/2 mice. The death of DCX^+ cells in WT mice is not surprising since most immature neurons die before they can be functionally integrated into the circuitry in both SVZ and SGZ of adult normal animals (Sun et al., 2004; Sierra et al., 2010). However, we failed to detect any apoptotic newborn cells in the striatum when stained with active caspase-3, an apoptotic marker (data not shown). It has been reported that apoptotic

newborn cells are cleared are rapidly cleared out through phagocytosis by unchallenged microglia present in the adult SGZ niche (Sierra et al., 2010) and apoptotic cells are phagocytosed within 1–2 hour from the start of apoptosis in most tissue (Savill, 1997). Therefore, the probability of detecting apoptotic newborn cells in our study could be very low. Nevertheless, the increased number of DCX^+ in R6/2 mice provides a therapeutic hope to replace the lost MSNs. Therefore, how to improve the survival of DCX^+ cells could be important. Neurotrophic factors play important roles in neuron development and survival. Reduced striatal BDNF has been shown in both HD patients (Ferrer et al., 2000) and transgenic models of HD (Zuccato and Cattaneo, 2009). The neurogenic effect of BDNF is well documented. For example, Infusion or adenoviral delivery of BDNF into ventricles induces SVZ proliferation and neurogenesis in the striatum of rodents (Benraiss et al., 2001; Pencea et al., 2001). In adult primates, adenoviral BDNF injected into the lateral ventricles promotes SVZ proliferation and migration of neuroblasts to the striatum (Bédard et al., 2006).

The behavioral benefits of elevated BDNF levels in the R6/1 and YAC128 HD mouse models have been well documented (Canals et al., 2004; Gharami et al., 2008; Xie et al., 2010). However, the effect of BDNF overexpression specifically on striatal neurogenesis in R6/2 mice has not been investigated. In the present study, we found that overexpression of BDNF in R6/2 mice increased the number of adult-born striatal neuroblasts 14 days after BrdU pulse labeling. We are not clear whether the increase is a result of more neuroblasts entering the striatum or prolonged survival. In fact, it is possible that both cascades play a role as BDNF has strong influenced on both proliferation and survival of neurons. In any event, we failed to detect any new mature neurons in the striatum of crossbred mice. We could not rule out the possibility that new neurons would be detected if we extended our study past 14 days after BrdU administration. However, it is more likely that striatal neuroblasts do not differentiate into neurons without considerable pharmacological intervention (Kohl et al., 2010; Luzzati et al., 2011). To overcome the non-permissive striatal microenvironment, it may be necessary to administer multiple factors that affect neurogenesis. For example, Cho et al. (2007) used adenoviral BDNF combined with adenoviral Noggin to stimulate striatal neurogenesis in the R6/2 model. Noggin, by inhibiting bone morphogenetic proteins, suppresses gliogenesis. The BDNF/Noggin combination delivered via adenovirus increased striatal neurogenesis, prolonged survival and delayed the onset of motor symptoms in R6/2 mice. Similar combinations of noggin and BDNF administration have been successfully used to induce new striatal neuron formation in rats (Chmielnicki et al., 2004; Benraiss et al., 2012).

3.3 Conclusion

In summary, our data indicate that BrdU-labeled newborn cells are increased in the striatum of R6/2 mice. These cells arise from two distinct populations of progenitor cells, OPCs in the striatum and neural stem cells in the SVZ and RMS. In postmortem human HD brain tissue, SVZ proliferation appears to be increased with the severity of the disease. Moreover, young neurons that co-express β-III tubulin and PCNA are found mainly in the deeper regions of subependymal layer adjacent to the caudate nucleus (Curtis et al., 2003). This data from adult human subjects highlights the clinical relevance of the study of neurogenesis in HD models including the findings presented here. However, it is still not clear whether these young neurons can migrate into the caudate nucleus and mature into functional neurons. In addition, changes in $NG2^+$ cells have not been investigated in HD patients. NG2-expressing cells represent an abundant population of progenitor cells throughout CNS that respond rapidly to brain damage. Compared to the relatively limited endogenous capacity for neuronal replacement, the therapeutic potential of modulating NG2-expressing cells should also be considered.

4. Experimental Procedure

4.1 Animals

All animal experiments were performed in accordance with the National Institutes of Health Guide for the Care and Use of Laboratory Animals and approved by the Institutional Animal Care and Use Committee of Florida Atlantic University (FAU). Breeding pairs of R6/2 transgenic mice [Strain #002810, (Mangiarini et al., 1996)] were purchased from the Jackson Laboratory (Bar Harbor, ME, USA), and the line was maintained by backcrossing to CBA/J C57BL/6J F1 in the animal facilities of FAU. *Bdnf* transgenic (BTg) mice under the control of the promoter for α-calcium/calmodulin-dependent protein kinase II were also obtained from the Jackson Laboratory [Strain #006579, (Huang et al., 1999)]. R6/2 mice were crossed to BTg mice to produce wild type (WT), BTg, R6/2 and BTg:R6/2 mice. Mice were maintained under temperature- and light-controlled conditions (20–23°C, 12/12-h light–dark cycle) with food and water ad libitum. DNA isolated from tail samples was used for routine genotyping. Both males and females were used in the studies.

4.2 BrdU labeling of newborn cells

Labeling of adult-born cells was performed by intraperitoneal (i.p.) injection of BrdU (Sigma, St Louis, USA). BrdU was dissolved in 0.9% saline solution at a concentration of 10 mg/ml. In the present study, we used two different BrdU-labeling paradigms (Fig. 1A and 1B). To examine cell differentiation and survival *in vivo* and ensure that infrequently dividing precursor cells would be labeled, 5-week-old R6/2 mice and WT littermates received daily injections of BrdU (50 mg/kg, i.p.) for 28 days. Two weeks after the last injection, animals at 11 weeks of age were euthanized by isoflurane inhalation, and transcardially perfused with 50 ml 0.9% saline followed by 50 ml 4% paraformaldehyde (PFA) in phosphate-buffered saline (PBS) (Fig. 1A). To examine SVZ proliferation and track the development of individual BrdU+ cells, we performed BrdU-pulse labeling experiments (Fig. 1B). Animals at 9 weeks old received a single injection of BrdU (100 mg/kg, i.p.) and were euthanized and perfusion-fixed 1 hour or 4 days after this single injection. Based on our pilot observation, it was hard to find striatal $BrdU^+$ cells at 7 or 14 days after a single injection. Accordingly, to increase the population of labeled cells at 7 and 14 days after injection, mice at 8 and 7 weeks old, respectively, received a series of four injections of BrdU (100 mg/kg, i.p.) in a single day at 2-hour intervals (total dose: 400 mg/kg) and were perfusion-fixed 7 or 14 days later. Therefore, in the pulse-labeling experiments, we gave a single BrdU injection to mice that were perfused 1 hour and 4 days later, but four injections at 2-hour intervals to mice that were perfused 7 and 14 days later. `All brain tissue was collected from mice at 9 weeks of age (Fig. 1B). For experiments using R6/2 mice crossed with BTg mice, mice were treated with a series of four BrdU in a single day at 2-hour intervals (4 × 100 mg/kg, i.p.) at 7 weeks of age and were perfusion-fixed 14 days later.

4.3 Immunofluorescence

After perfusion-fixation, brains were dissected, post-fixed in 4% PFA overnight at 4°C and cryopreserved with 30% sucrose in PBS overnight at 4°C. Brains were then rapidly frozen in optimal cutting temperature compound (OCT, Sakura) in a dry ice/acetone bath. Sagittal sections of 30 μm thickness were cut using a Microm cryostat and every 12^{th} section throughout the entire striatum in one hemisphere was collected and processed for immunofluorescence as described below. Sections were stored at −20°C in antigen preservation solution (1% polyvinyl pyrrolidone, 50% ethylene glycol in PBS) prior to processing (Burke et al., 2009).

Free-floating sections were blocked in blocking buffer [10% normal goat serum, 1% bovine serum albumin (BSA), 0.3% Triton X-100 in PBS] for 1 hour at room temperature. Sections

were then incubated with cell type-specific markers overnight at 4°C. The following cell-type specific markers were used: rabbit polyclonal anti-Olig2 (Cat #AB9610, 1:400, Millipore, Temecula, CA), rabbit polyclonal anti-doublecortin (Cat #4604, 1:400, Cell Signaling Technologies, Danvers, MA), mouse monoclonal anti-NeuN (Cat #MAB377, 1:400, Millipore), rabbit polyclonal anti-calretinin, (Cat #AB149, 1:500, Chemicon), mouse monoclonal anticalbindin D-28K (Cat #C9848, 1:500, Sigma), mouse monoclonal anti-CNPase (Cat #MAB326, 1:400, Millipore), rabbit polyclonal anti-NG2 (Cat #MAB5320, 1:400, Millipore), mouse monoclonal anti-S100p (Cat #CB1040, 1:400, Millipore), rabbit polyclonal anti-GFAP (Cat #AB5804, 1:400, Millipore), rabbit polyclonal anti-Iba1 (Cat# 019-19741, 1:500, Wako, Osaka, Japan). After incubation with primary antibodies, sections were extensively washed with PBS and further incubated with species-appropriate Alexa Fluor-conjugated secondary IgGs (1:2000, Invitrogen, Carlsbad, CA) overnight at 4°C.

For co-localization of cell marker with $BrdU^+$ or $PCNA^+$ cells, a two-step staining procedure was used. Tissue sections processed with primary antibodies against different cell-type specific markers as above were then subjected to antigen retrieval which included incubation in 2N HCl for 30 minutes at 37°C followed by washing in 0.1 M borate buffer (pH=8.5). Sections were stained with rat anti-BrdU antibodies (Cat #MCA2060T, 1:500, AbD Serotec, Raleigh, NC) or mouse monoclonal anti-PCNA (Cat #sc-25280, 1:500, Santa Cruz Biotechnology, Santa Cruz, CA) overnight at 4°C, followed by incubating with species-appropriate Alexa Fluor-conjugated secondary IgGs (1:2000, Invitrogen) overnight at 4°C. After extensive wash with PBS, the sections were mounted on silane-coated microscope slides with Prolong Gold antifade reagent (Invitrogen). Fluorescent signals in the selected area of the striatum (Fig. 1B) were examined and images were collected using a Zeiss LSM700 laser-scanning microscope or a Zeiss AxioImager D1 epifluorescent microscope. Images brightness and contrast were made in Zen software and figures were assembled in Adobe Illustrator CS5.

4.4 Image analysis and data quantification

The densities of $BrdU^+$ cells (number of cells/mm^3) in the dorsal striatum of WT and R6/2 mice (Fig. 1C) after long-term BrdU treatment were determined as follows. Z-stack images (320 μm × 320 μm × 24 μm) from three randomly selected areas in the striatum were obtained for each tissue section at 40X oil objective magnification (NA 1.3) using a Zeiss LSM700 confocal laser-scanning microscope. Initially, we randomly superimposed each stack image with a 40 μm × 40 μm grid using the particle analysis plugin from NIH ImageJ. The numbers of BrdU-immunopositive cells were counted in each grid of the Z-stack image following the optical dissector method as described (West et al., 1991). The depth of the optical sector is set at 20 μm to exclude the uneven surface of the slices. Therefore, the volume of the dissector is 40 μm × 40 μm × 20 μm = 32000 μm^3 . Mean counts for individual sections were used to generate the mean density of $BrdU^+$ cells in striatum of each animal (cells/mm^3), and these values were used to calculate group mean values ± the standard error of the mean (SEM).

For the BrdU pulse-labeling experiments, we counted the number of $BrdU^+$ cells per striatum due to the low number of cells that were labeled. Striatal images were first taken at 4x objective magnification (NA 0.13) on a Zeiss AxioImager epifluorescent scope and $BrdU^+$ cells in every 12^{th} section throughout the entire striatum in one hemisphere were counted by an experimenter blind to the subject's genotype. The numbers were combined for each striatum and averaged for each animal. The data were expressed as absolute number of cells per striatum. For counts of double-labeled cells, striatal sections were examined at 40x magnification. The co-localization was later confirmed by orthogonal views. Additionally, for each $BrdU^+/Olig2^+$ and $BrdU^+/DCX^+$ cells, its vertical distance (μm) from the later ventricle (LV) and corpus callosum (CC) were measured using Zeiss AxioVision

analysis software 4.7. To quantify SVZ cell proliferation, the SVZ in each imaged section (n=12 for each animal) was outlined and the area was calculated using the Zeiss AxioVision imaging software 4.7. The number of BrdU+ nuclei in the SVZ of each section was counted at 20X magnification. The mean density of $BrdU^+$ cells in the SVZ was then calculated from section means for each animal and expressed as number of cells/mm^2 .

4.5 Data analysis

All data are expressed as group (genotype) means ± S.E.M. To establish significance, group mean comparisons were performed with unpaired, two-tailed Student's t-test using GraphPad Prism 5.0 (San Diego, CA, USA). The criterion for significance was set at $p < 0.05$.

Supplementary Material

Refer to Web version on PubMed Central for supplementary material.

Acknowledgments

This work was supported by the National Institute of Neurological Disorders and Stroke [R15NS066339 to JW].

Abbreviations

BDNF	brain derived neurotrophic factor
BrdU	5-bromo-2-deoxyuridine
BSA	bovine serum albumin
BTg	BDNF-overexpressing transgenic mice
CR	calretinin
CC	corpus collosum
CNPase	2,3-cyclic nucleotide 3-phosphodiesterase
DCX	doublecortin
HD	Huntington's disease
i.p.	intraperitoneal
LV	lateral ventricle
MSNs	medium spiny neurons
NeuN	neuronal nuclei
Olig2	oligodendrocyte lineage transcription factor 2
OPCs	oligodendroglial progenitor cells
PBS	phosphate-buffered saline
PFA	paraformaldehyde
RMS	rostral migratory stream
SVZ	subventricular zone
WT	wild type

References

Arvidsson A, Collin T, Kirik D, Kokaia Z, Lindvall O. Neuronal replacement from endogenous precursors in the adult brain after stroke. Nat. Med. 2002; 8:963–970. [PubMed: 12161747]

Bartzokis G, Lu PH, Tishler TA, Fong SM, Oluwadara B, Finn JP, Huang D, Bordelon Y, Mintz J, Perlman S. Myelin breakdown and iron changes in Huntington's disease: pathogenesis and treatment implications. Neurochem. Res. 2007; 32:1655–1664. [PubMed: 17484051]

Batista CMC, Kippin TE, Willaime-Morawek S, Shimabukuro MK, Akamatsu W, van der Kooy D. A progressive and cell non-autonomous increase in striatal neural stem cells in the Huntington's disease R6/2 mouse. Journal of Neuroscience. 2006; 26:10452–10460. [PubMed: 17035529]

Benraiss A, Bruel-Jungerman E, Lu G, Economides AN, Davidson B, Goldman SA. Sustained induction of neuronal addition to the adult rat neostriatum by AAV4-delivered noggin and BDNF. Gene Ther. 2012; 19:483–493. [PubMed: 21918547]

Benraiss A, Chmielnicki E, Lerner K, Roh D, Goldman SA. Adenoviral brain-derived neurotrophic factor induces both neostriatal and olfactory neuronal recruitment from endogenous progenitor cells in the adult forebrain. Journal of Neuroscience. 2001; 21:6718–6731. [PubMed: 11517261]

Benraiss A, Goldman SA. Cellular therapy and induced neuronal replacement for Huntington's disease. Neurotherapeutics. 2011; 8:577–590. [PubMed: 21971961]

Bergles DE, Roberts JD, Somogyi P, Jahr CE. Glutamatergic synapses on oligodendrocyte precursor cells in the hippocampus. Nature. 2000; 405:187–191. [PubMed: 10821275]

Bédard A, Gravel C, Parent A. Chemical characterization of newly generated neurons in the striatum of adult primates. Exp Brain Res. 2006; 170:501–512. [PubMed: 16328260]

Brandt MD, Jessberger S, Steiner B, Kronenberg G, Reuter K, Bick-Sander A, Behrens von der W, Kempermann G. Transient calretinin expression defines early postmitotic step of neuronal differentiation in adult hippocampal neurogenesis of mice. Mol. Cell. Neurosci. 2003; 24:603–613.

Burke MW, Zangenehpour S, Ptito M. Brain banking: making the most of your research specimens. J Vis Exp. 2009

Busch SA, Horn KP, Cuascut FX, Hawthorne AL, Bai L, Miller RH, Silver J. Adult NG2+ Cells Are Permissive to Neurite Outgrowth and Stabilize Sensory Axons during Macrophage-Induced Axonal Dieback after Spinal Cord Injury. Journal of Neuroscience. 2010; 30:255–265. [PubMed: 20053907]

Canals JM, Pineda JR, Torres-Peraza JF, Bosch M, Martín-Ibañez R, Muñoz MT, Mengod G, Ernfors P, Alberch J. Brain-derived neurotrophic factor regulates the onset and severity of motor dysfunction associated with enkephalinergic neuronal degeneration in Huntington's disease. Journal of Neuroscience. 2004; 24:7727–7739. [PubMed: 15342740]

Chmielnicki E, Benraiss A, Economides AN, Goldman SA. Adenovirally expressed noggin and brain-derived neurotrophic factor cooperate to induce new medium spiny neurons from resident progenitor cells in the adult striatal ventricular zone. Journal of Neuroscience. 2004; 24:2133–2142. [PubMed: 14999064]

Cho S-R, Benraiss A, Chmielnicki E, Samdani A, Economides A, Goldman SA. Induction of neostriatal neurogenesis slows disease progression in a transgenic murine model of Huntington disease. J. Clin. Invest. 2007; 117:2889–2902. [PubMed: 17885687]

Clarke LE, Young KM, Hamilton NB, Li H, Richardson WD, Attwell D. Properties and fate of oligodendrocyte progenitor cells in the corpus callosum, motor cortex, and piriform cortex of the mouse. Journal of Neuroscience. 2012; 32:8173–8185. [PubMed: 22699898]

Curtis MA, Eriksson PS, Faull RLM. Progenitor cells and adult neurogenesis in neurodegenerative diseases and injuries of the basal ganglia. Clin. Exp. Pharmacol. Physiol. 2007; 34:528–532. [PubMed: 17439428]

Curtis MA, Penney EB, Pearson AG, van Roon-Mom WMC, Butterworth NJ, Dragunow M, Connor B, Faull RLM. Increased cell proliferation and neurogenesis in the adult human Huntington's disease brain. Proc. Natl. Acad. Sci. U.S.A. 2003; 100:9023–9027. [PubMed: 12853570]

Eriksson PS, Perfilieva E, Björk-Eriksson T, Alborn AM, Nordborg C, Peterson DA, Gage FH. Neurogenesis in the adult human hippocampus. Nat. Med. 1998; 4:1313–1317. [PubMed: 9809557]

Ferrer I, Goutan E, Marín C, Rey MJ, Ribalta T. Brain-derived neurotrophic factor in Huntington disease. Brain Res. 2000; 866:257–261. [PubMed: 10825501]

Gharami K, Xie Y, An JJ, Tonegawa S, Xu B. Brain-derived neurotrophic factor over-expression in the forebrain ameliorates Huntington's disease phenotypes in mice. J. Neurochem. 2008; 105:369–379. [PubMed: 18086127]

Gil JMAC, Mohapel P, Araújo IM, Popovic N, Li J-Y, Brundin P, Petersén A. Reduced hippocampal neurogenesis in R6/2 transgenic Huntington's disease mice. Neurobiol. Dis. 2005; 20:744–751. [PubMed: 15951191]

Gil-Mohapel J, Simpson JM, Ghilan M, Christie BR. Neurogenesis in Huntington's disease: can studying adult neurogenesis lead to the development of new therapeutic strategies? Brain Res. 2011; 1406:84–105. [PubMed: 21742312]

Gómez-Tortosa E, MacDonald ME, Friend JC, Taylor SA, Weiler LJ, Cupples LA, Srinidhi J, Gusella JF, Bird ED, Vonsattel JP, Myers RH. Quantitative neuropathological changes in presymptomatic Huntington's disease. Ann. Neurol. 2001; 49:29–34. [PubMed: 11198293]

Han I, You Y, Kordower JH, Brady ST, Morfini GA. Differential vulnerability of neurons in Huntington's disease: the role of cell type-specific features. J. Neurochem. 2010; 113:1073–1091. [PubMed: 20236390]

Huang ZJ, Kirkwood A, Pizzorusso T, Porciatti V, Morales B, Bear MF, Maffei L, Tonegawa S. BDNF regulates the maturation of inhibition and the critical period of plasticity in mouse visual cortex. Cell. 1999; 98:739–755. [PubMed: 10499792]

Kernie SG, Parent JM. Forebrain neurogenesis after focal Ischemic and traumatic brain injury. Neurobiol. Dis. 2010; 37:267–274. [PubMed: 19909815]

Kohl Z, Regensburger M, Aigner R, Kandasamy M, Winner B, Aigner L, Winkler J. Impaired adult olfactory bulb neurogenesis in the R6/2 mouse model of Huntington's disease. BMC Neurosci. 2010; 11:114. [PubMed: 20836877]

Lazic SE, Grote H, Armstrong RJE, Blakemore C, Hannan AJ, van Dellen A, Barker RA. Decreased hippocampal cell proliferation in R6/1 Huntington's mice. Neuroreport. 2004; 15:811–813. [PubMed: 15073520]

Lazic SE, Grote HE, Blakemore C, Hannan AJ, van Dellen A, Phillips W, Barker RA. Neurogenesis in the R6/1 transgenic mouse model of Huntington's disease: effects of environmental enrichment. Eur. J. Neurosci. 2006; 23:1829–1838. [PubMed: 16623840]

Lie DC, Song H, Colamarino SA, Ming G-L, Gage FH. Neurogenesis in the adult brain: new strategies for central nervous system diseases. Annu. Rev. Pharmacol. Toxicol. 2004; 44:399–421. [PubMed: 14744252]

Luzzati F, De Marchis S, Parlato R, Gribaudo S, Schütz G, Fasolo A, Peretto P. New striatal neurons in a mouse model of progressive striatal degeneration are generated in both the subventricular zone and the striatal parenchyma. PLoS ONE. 2011; 6:e25088. [PubMed: 21980380]

Mangiarini L, Sathasivam K, Seller M, Cozens B, Harper A, Hetherington C, Lawton M, Trottier Y, Lehrach H, Davies SW, Bates GP. Exon 1 of the HD gene with an expanded CAG repeat is sufficient to cause a progressive neurological phenotype in transgenic mice. Cell. 1996; 87:493–506. [PubMed: 8898202]

Ming G-L, Song H. Adult neurogenesis in the mammalian central nervous system. Annu. Rev. Neurosci. 2005; 28:223–250. [PubMed: 16022595]

Myers RH, Vonsattel JP, Paskevich PA, Kiely DK, Stevens TJ, Cupples LA, Richardson EP, Bird ED. Decreased neuronal and increased oligodendroglial densities in Huntington's disease caudate nucleus. J. Neuropathol. Exp. Neurol. 1991; 50:729–742. [PubMed: 1836225]

Ohira K. Injury-induced neurogenesis in the mammalian forebrain. Cell. Mol. Life Sci. 2011; 68:1645–1656. [PubMed: 21042833]

Paoletti P, Vila I, Rifé M, Lizcano JM, Alberch J, Ginés S. Dopaminergic and glutamatergic signaling crosstalk in Huntington's disease neurodegeneration: the role of p25/cyclin-dependent kinase 5. Journal of Neuroscience. 2008; 28:10090–10101. [PubMed: 18829967]

Pencea V, Bingaman KD, Wiegand SJ, Luskin MB. Infusion of brain-derived neurotrophic factor into the lateral ventricle of the adult rat leads to new neurons in the parenchyma of the striatum,

septum, thalamus, and hypothalamus. Journal of Neuroscience. 2001; 21:6706–6717. [PubMed: 11517260]

Phillips W, Morton AJ, Barker RA. Abnormalities of neurogenesis in the R6/2 mouse model of Huntington's disease are attributable to the in vivo microenvironment. Journal of Neuroscience. 2005; 25:11564–11576. [PubMed: 16354914]

Polito A, Reynolds R. NG2-expressing cells as oligodendrocyte progenitors in the normal and demyelinated adult central nervous system. J. Anat. 2005; 207:707–716. [PubMed: 16367798]

Reiner A, Albin RL, Anderson KD, D'Amato CJ, Penney JB, Young AB. Differential loss of striatal projection neurons in Huntington disease. Proc. Natl. Acad. Sci. U.S.A. 1988; 85:5733–5737. [PubMed: 2456581]

Richardson WD, Young KM, Tripathi RB, McKenzie I. NG2-glia as multipotent neural stem cells: fact or fantasy? Neuron. 2011; 70:661–673. [PubMed: 21609823]

Rosas HD, Lee SY, Bender AC, Zaleta AK, Vangel M, Yu P, Fischl B, Pappu V, Onorato C, Cha JH, Salat DH, Hersch SM. Altered white matter microstructure in the corpus callosum in Huntington's disease: implications for cortical “disconnection”. Neuroimage. 2010; 49:2995–3004. [PubMed: 19850138]

Saha B, Jaber M, Gaillard A. Potentials of endogenous neural stem cells in cortical repair. Front Cell Neurosci. 2012; 6:14. [PubMed: 22509153]

Savill J. Recognition and phagocytosis of cells undergoing apoptosis. Br. Med. Bull. 1997; 53:491–508. [PubMed: 9374033]

Sierra A, Encinas JM, Deudero JJP, Chancey JH, Enikolopov G, Overstreet-Wadiche LS, Tsirka SE, Maletic-Savatic M. Microglia shape adult hippocampal neurogenesis through apoptosis-coupled phagocytosis. Cell Stem Cell. 2010; 7:483–495. [PubMed: 20887954]

Simpson JM, Gil-Mohapel J, Pouladi MA, Ghilan M, Xie Y, Hayden MR, Christie BR. Altered adult hippocampal neurogenesis in the YAC128 transgenic mouse model of Huntington disease. Neurobiol. Dis. 2011; 41:249–260. [PubMed: 20875859]

Sun W, Winseck A, Vinsant S, Park O-H, Kim H, Oppenheim RW. Programmed cell death of adult-generated hippocampal neurons is mediated by the proapoptotic gene Bax. Journal of Neuroscience. 2004; 24:11205–11213. [PubMed: 15590937]

Tattersfield AS, Croon RJ, Liu YW, Kells AP, Faull RLM, Connor B. Neurogenesis in the striatum of the quinolinic acid lesion model of Huntington's disease. Neuroscience. 2004; 127:319–332. [PubMed: 15262322]

West MJ, Slomianka L, Gundersen HJ. Unbiased stereological estimation of the total number of neurons in thesubdivisions of the rat hippocampus using the optical fractionator. Anat. Rec. 1991; 231:482–497. [PubMed: 1793176]

Winner B, Kohl Z, Gage FH. Neurodegenerative disease and adult neurogenesis. Eur. J. Neurosci. 2011; 33:1139–1151. [PubMed: 21395858]

Xiang Z, Valenza M, Cui L, Leoni V, Jeong H-K, Brilli E, Zhang J, Peng Q, Duan W, Reeves SA, Cattaneo E, Krainc D. Peroxisome-proliferator-activated receptor gamma coactivator 1 **a** contributes to dysmyelination in experimental models of Huntington's disease. Journal of Neuroscience. 2011; 31:9544–9553. [PubMed: 21715619]

Xie Y, Hayden MR, Xu B. BDNF overexpression in the forebrain rescues Huntington's disease phenotypes in YAC128 mice. Journal of Neuroscience. 2010; 30:14708–14718. [PubMed: 21048129]

Zhao C, Deng W, Gage FH. Mechanisms and functional implications of adult neurogenesis. Cell. 2008; 132:645–660. [PubMed: 18295581]

Zuccato C, Cattaneo E. Brain-derived neurotrophic factor in neurodegenerative diseases. Nat Rev Neurol. 2009; 5:311–322. [PubMed: 19498435]

Zuccato C, Valenza M, Cattaneo E. Molecular mechanisms and potential therapeutical targets in Huntington's disease. Physiol. Rev. 2010; 90:905–981. [PubMed: 20664076]

Highlights

- Compared to WT mice, R6/2 mice exhibit a two-fold increase in $BrdU^+$ striatal cells.
- The phenotypes of striatal $BrdU^+$ cells were identified using specific markers.
- Overexpression of BDNF in R6/2 mice increased the number of striatal neuroblasts.
- Functional implications of the increase in striatal $BrdU^+$ cells are discussed.

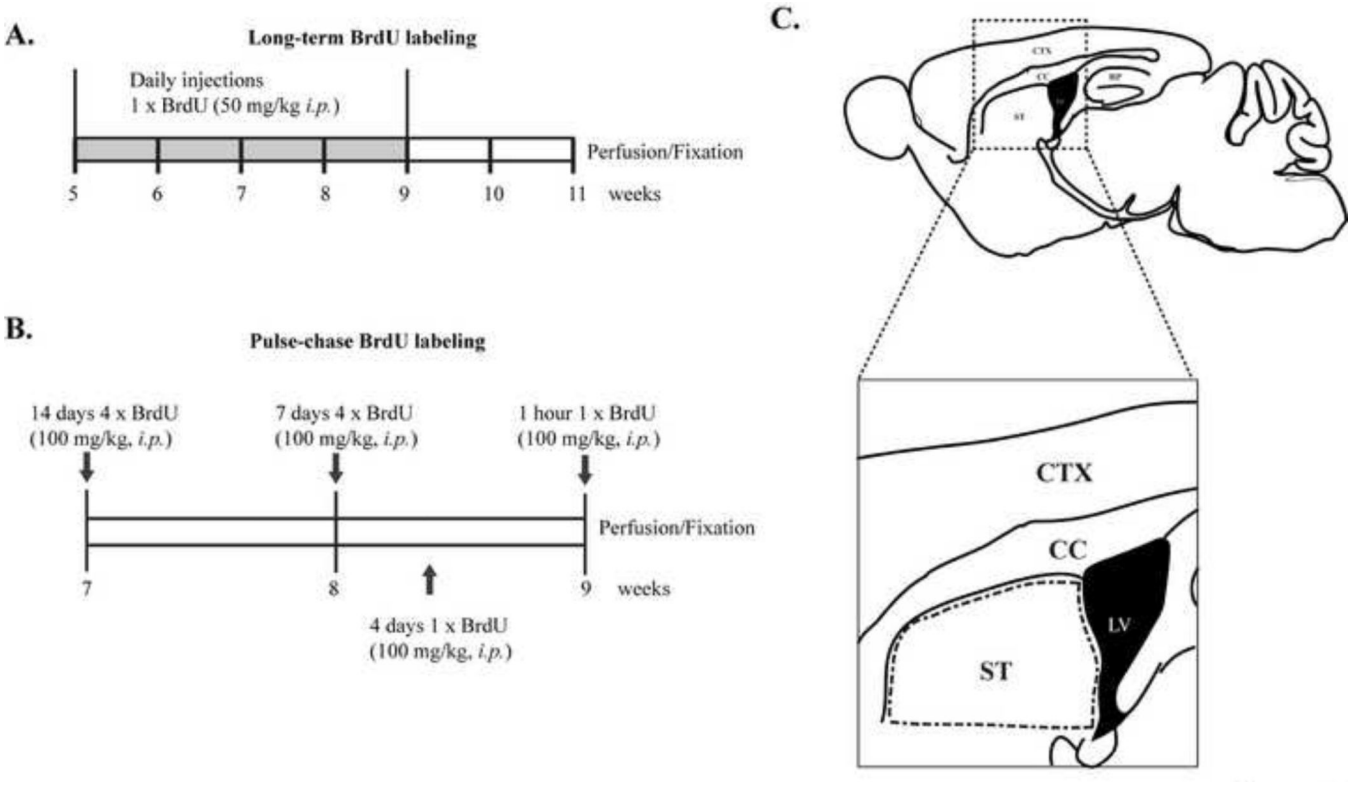

Figure 1.

Method for labeling and counting newborn cells in adult mouse striatum. Experimental design showing (A) long-term BrdU labeling and (B) pulse BrdU labeling. C. Schematic drawing of a sagittal mouse section. $BrdU^+$ cells were identified and counted in a defined region of the dorsal striatum adjacent to the SVZ (outlined in dashed lines). ST, striatum; LV, lateral ventricle; CC, corpus callosum; CTX, cortex.

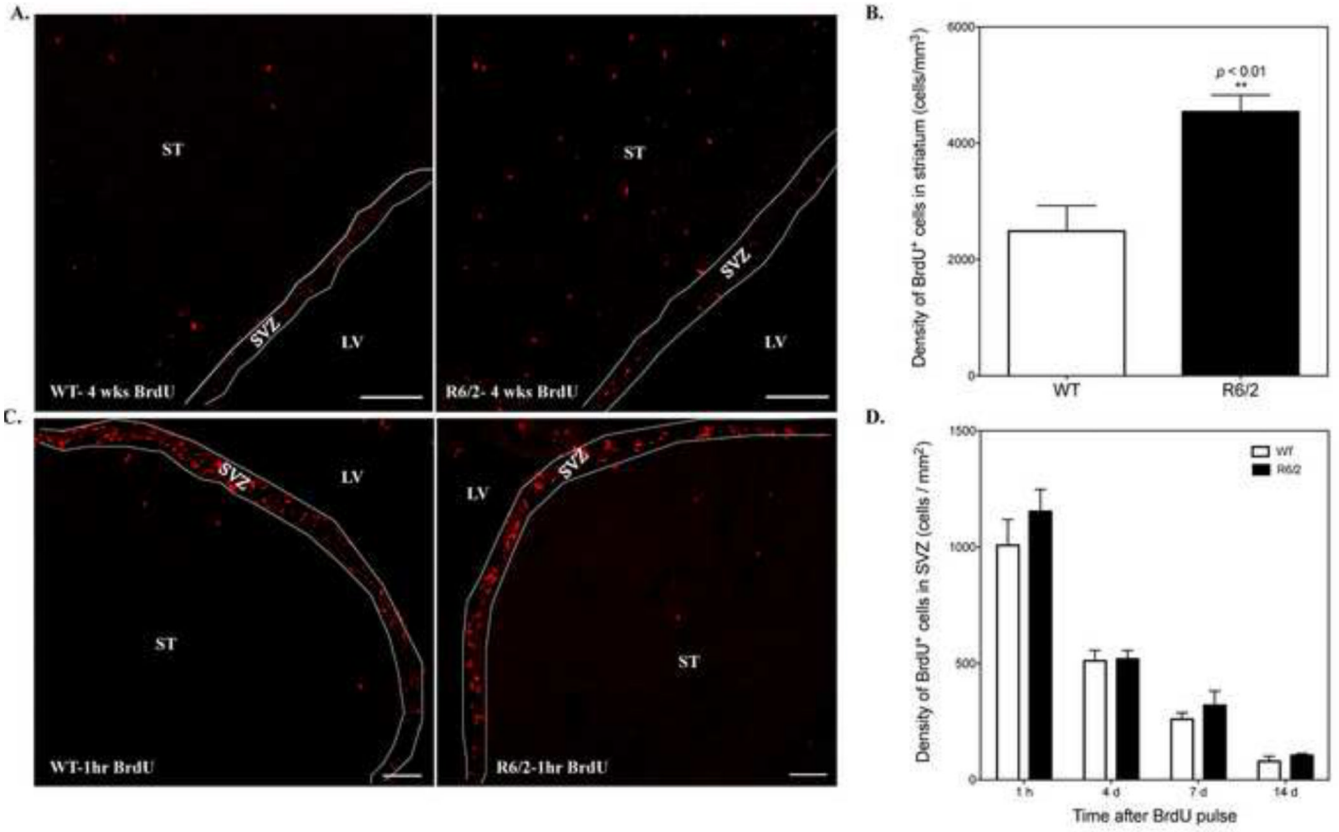

Figure 2.

R6/2 mice show increased number of adult-born striatal cells with no change in SVZ proliferation when compared to WT mice. A. Representative confocal images of $BrdU^+$ cells in the striatum of WT and R6/2 mice at 11 weeks of age after long-term BrdU labeling. Scale bar: 100 μm. B. Quantification of $BrdU^+$ cells in the striatum of WT (n=4) and R6/2 (n=5) mice at 11 weeks old after long-term labeling. $^{**}p<0.01$, student's t-test. C. Representative confocal images of $BrdU^+$ cells in the striatum and SVZ of 9-week-old WT and R6/2 mice 1-hour post-BrdU injection. Scale bar: 100 um. LV, lateral ventricle; ST, striatum; SVZ, subventricular zone. D.The density of $BrdU^+$ cells in the SVZ of WT and R6/2 mice at 1 hour, 4 days, 7 days and 14 days following BrdU pulse injections (for each time point, WT, n=3; R6/2, n=3).

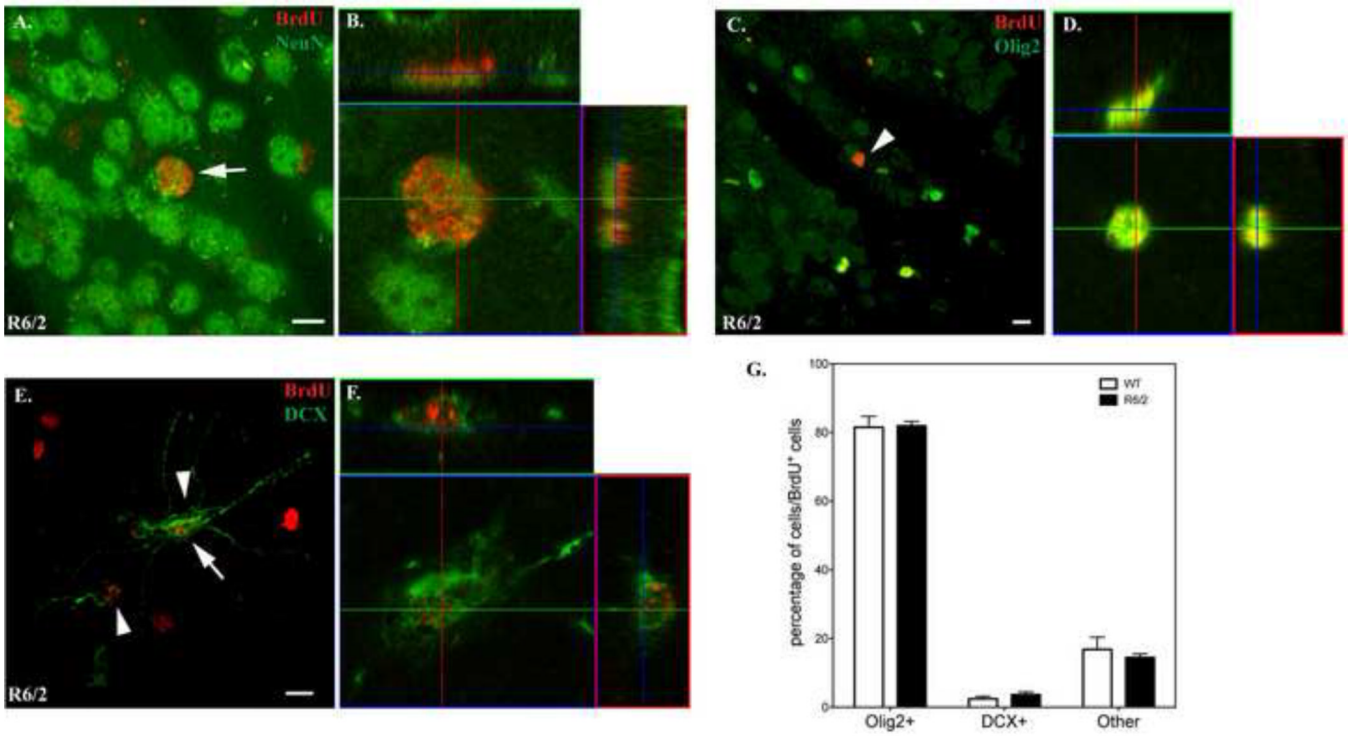

Figure 3.

Identification of $BrdU^+$ cells in the striatum of WT and R6/2 mice at 11 weeks of age with cell-type specific markers. Images were taken in z-stacks with a 63x oil objective (NA 1.40) on a Zeiss LSM700 confocal microscope. A-B. $BrdU^+$ cells are not co-labeled with NeuN. The arrow indicates a striatal $BrdU^+$ cell in R6/2 mice that was not co-localized with NeuN as demonstrated by the orthogonal view (B). C-D. A representative image showing $BrdU^+$ cells that co-express Olig2 in the striatum of R6/2 mice (arrowheads). The orthogonal view of a $BrdU^+/Olig2^+$ cell (indicated by an arrow in C) is shown in (D). E-F. A representative image showing $BrdU^+$ cells that co-express DCX in the striatum of R6/2 mice (arrowheads). The orthogonal view of a $BrdU^+/DCX^+$ cell (indicated by an arrow in E) is shown in (F). A, C and E are maximum intensity projections of the z-stack images. Scale bar: 10 μm. G. Quantitative analysis of the percentage of each cell type in $BrdU^+$ cells. The "Other" category includes GFAP-, Iba-, $S100\beta^+$ and other cell types not investigated in this study.

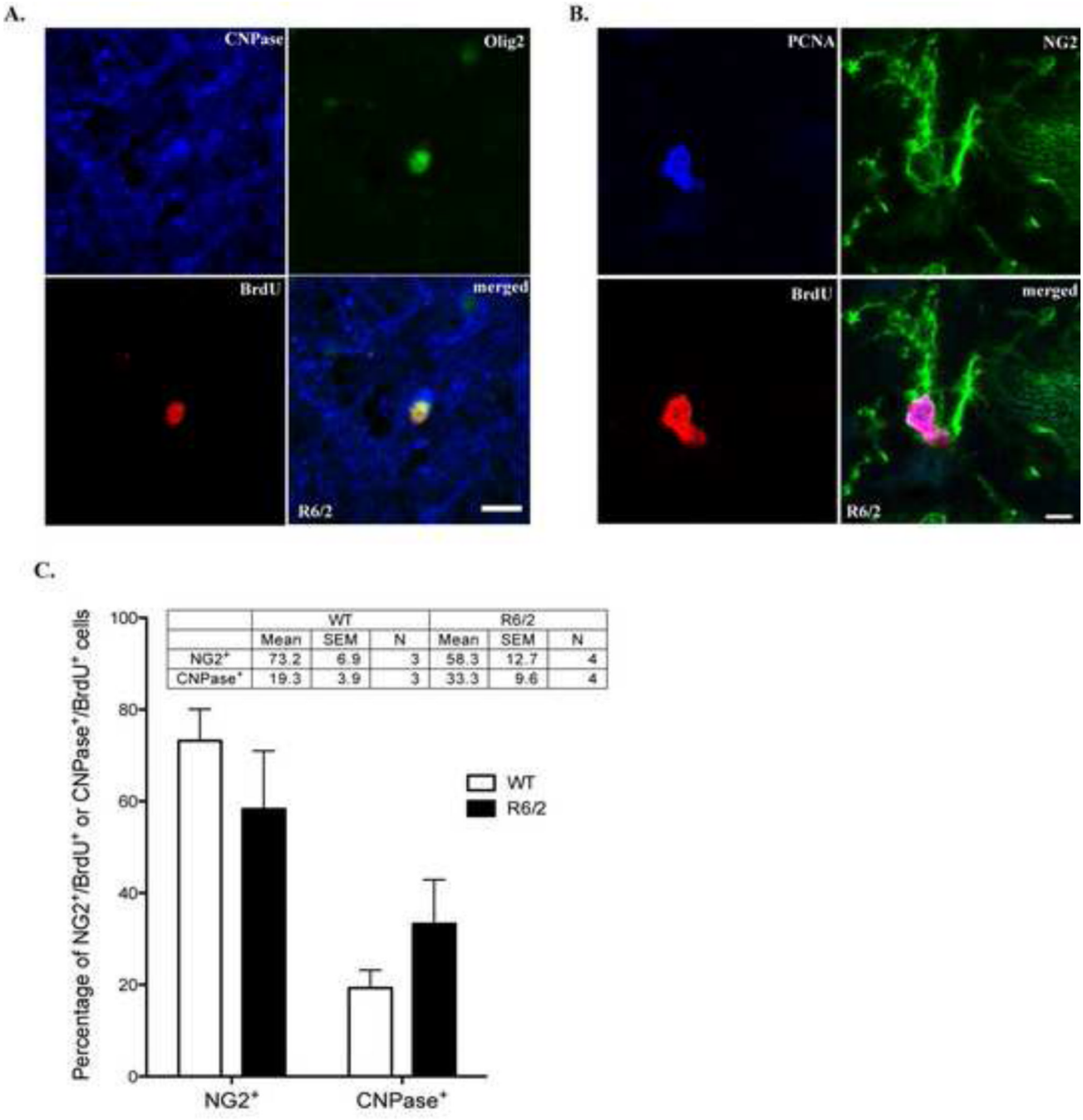

	WT			R6/2		
	Mean	SEM	N	Mean	SEM	N
NG2+	73.2	6.9	3	58.3	12.7	4
CNPase+	19.3	3.9	3	33.3	9.6	4

Figure 4.

Striatal Olig2$^+$ cells represent mature oligodendrocytes or OPCs. A. A representative confocal image showing a newborn Olig2$^+$ cell in an 11-week-old R6/2 mouse as a mature oligodendrocyte that co-express BrdU, Olig2 and CNPase. Scale bar: 10 um. B. A representative confocal image showing newborn cells in an 11-week-old R6/2 mouse as OPCs that co-express BrdU, NG2 and PCNA. Scale bar: 5 μm. C. Statistical analysis of the percentage of newly formed NG2$^+$ or CNPase$^+$ striatal in WT and R6/2 mice after long-term BrdU treatment.

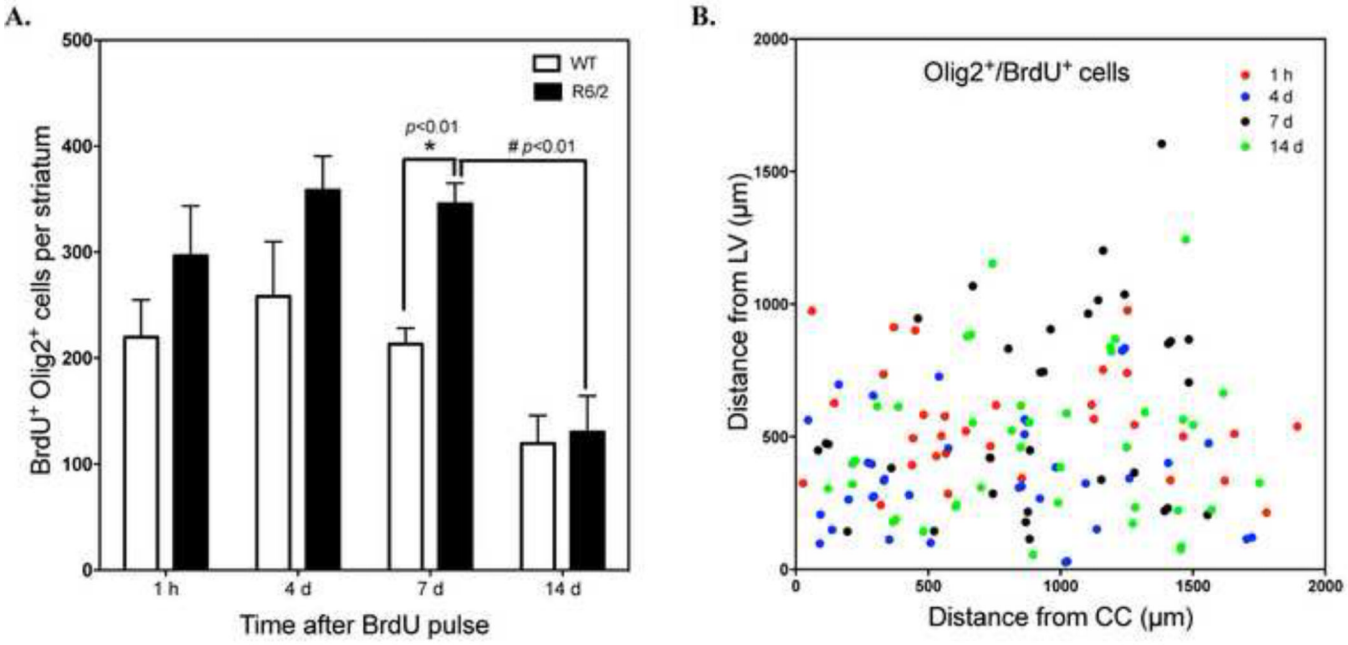

Figure 5.

$BrdU^+/Oligo2^+$ cells arise from intrinsic progenitors in both WT and R6/2 mice. A. Number of $BrdU^+/Olig2^+$ cells in the striatum of WT and R6/2 mice at 1 hour, 4 days, 7 days and 14 days after BrdU pulse labeling (for each time point, WT, n=3; R6/2, n=3). *p<0.01, R6/2 mice at 7 days *vs.* WT mice at 7 days; #p<0.01, R6/2 mice at 14 days *vs.* R6/2 mice at 7 days, student's t-test. B. The relative position of $BrdU^+/Olig2^+$ cells in the striatum of R6/2 mice at different time points were estimated by measuring cell distances from the LV and CC.

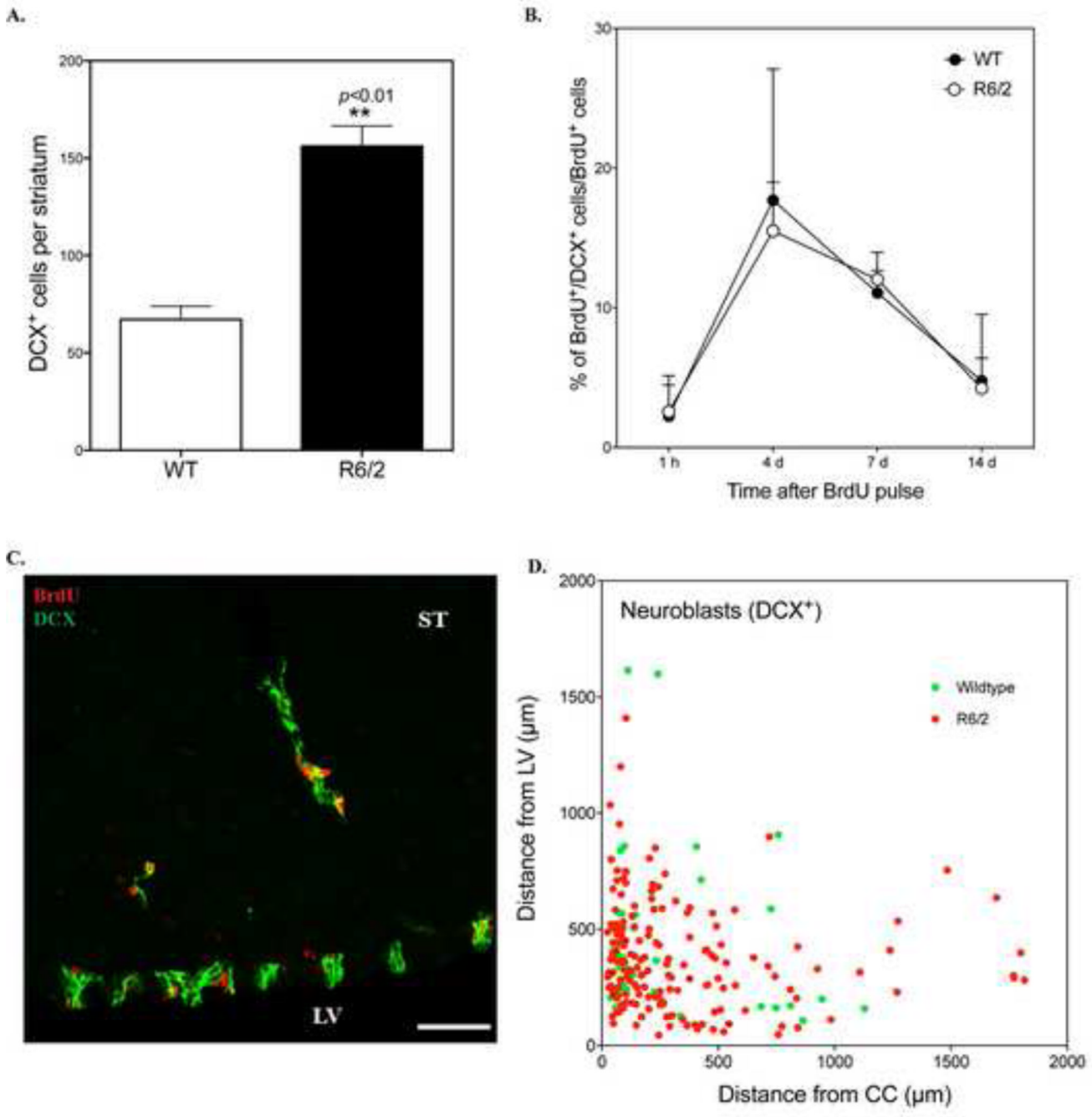

Figure 6.

The number of striatal DCX^+ cells is increased in R6/2 mice and originate from SVZ. A. Quantitative analysis of the number of neuroblasts in the striatum of WT and R6/2 mice at 9 weeks old (n=12 for each group). B. Percentage of $BrdU^+$ cells that co-express DCX at different time points after BrdU pulse labeling. C. A representative confocal image showing that $DCX^+/BrdU^+$ cells formed migrating clusters in the striatum of R6/2 mice. LV: lateral ventricle, ST: striatum. Scale bar: 50 µm. D. The relative position of DCX^+ cells in the striatum of R6/2 and WT mice at 14 days after BrdU pulse labeling were estimated by measuring cell distance from the LV and CC.

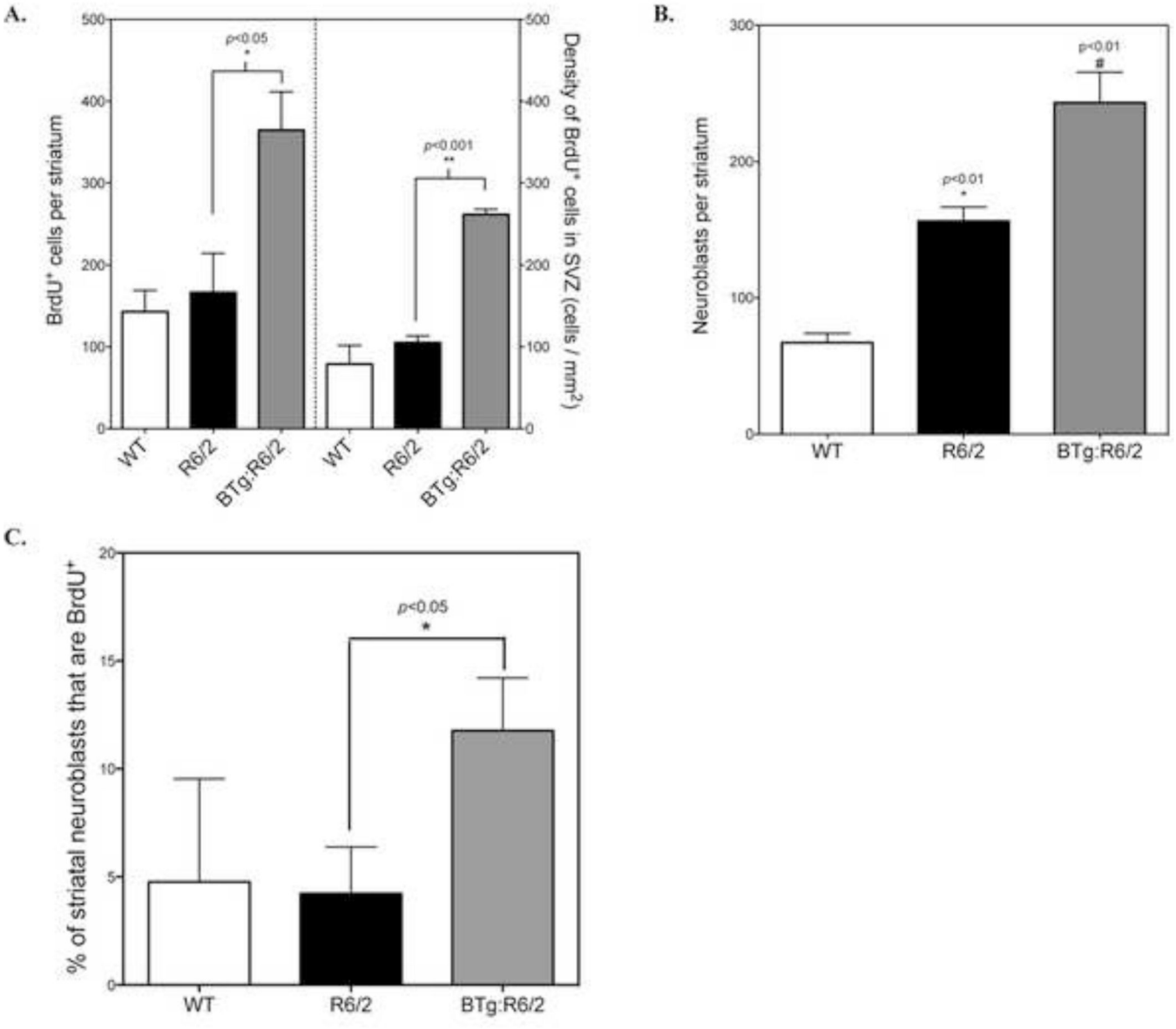

Figure 7.

Overexpression of BDNF increases the number of DCX^+ cells in the striatum of R6/2 mice at 14 days post-BrdU injection. WT (n=3), R6/2 (n=3) and BTg:R6/2 mice (n=4) received 4 × BrdU (100 mg/kg, *i.p.* 2 hours apart) in a day and perfuse-fixed 14 days later. A. Quantitative analysis of the $BrdU^+$ cells in the striatum and SVZ. *p<0.05, **p<0.001, BTg:R6/2 mice *vs.* R6/2 mice, student's t-test. B. Quantitative analysis of the DCX^+ cells in the striatum. *p<0.01, R6/2 mice vs. WT mice; #p<0.01, BTg:R6/2 mice *vs.* R6/2 mice, student's t-test. C. Percentage of $BrdU^+$ cells that co-express DCX in the striatum. *p<0.05, BTg:R6/2 mice *vs.* R6/2 mice, student's *t*-test.